N86-17843

GALLIUM ARSENIDE SOLAR CELL EFFICIENCY - PROBLEMS AND POTENTIAL

V.G. Weizer and M.P. Godlewski
NASA Lewis Research Center
Cleveland, Ohio

Under ideal conditions the GaAs solar cell should be able to operate at an AMO efficiency exceeding 27 percent (ref. 1), whereas to date the best measured efficiencies barely exceed 19 percent. Of more concern is the fact that there has been no improvement in the past half decade, despite the expenditure of considerable effort. The present paper analyzes state-of-the-art GaAs efficiency in an attempt to determine the feasibility of improving on the status quo. We will first consider the possible gains to be had in the planar cell, and then attempt to predict the efficiency levels that could be achieved with a grating geometry.

THE PLANAR CELL

The best efforts of the eight laboratories most involved in the development of the GaAs solar cell are listed in table I. The N-base cells are all basically similar in construction in that they have a passivating P-type AlGaAs window layer deposited on the emitter surface. The P-base MIT cell, on the other hand, uses an AlGaAs layer to form a heteroface BSF structure. The N-base cells appear to have a slight efficiency edge over the P-base devices.

E-2706-5

Figure 1 is a plot of the N-base cell short circuit current as a function of AlGaAs window thickness. These cells are quite different in their externals (AR coatings, window thicknesses, etc.). In order to get an idea of their relative internal perfection we calculated the short circuit densities expected from each of them assuming 100 percent internal collection efficiency, and compared this value with that actually achieved. When we did this, Hughes cell 2598 stood out from the rest in that its measured J_{sc} coincided with that calculated assuming a 100 percent internal collection efficiency. This indicates, among other things, that the Hughes group has succeeded in reducing the AlGaAs-GaAs interface recombination velocity IRV at least an order of magnitude lower than the emitter diffusion velocity ($\leq$0.1 D/L).

However, even though this cell is internally perfect, it has several external problems. It has a thick (0.5 μm) window and a 10 percent shadowing loss due to the front grid coverage. The solid curve in figure 1 indicates the J_{sc} increases that would accompany a reduction in window thickness. The dashed curve indicates the gains possible if the grid coverage were reduced to 5 percent. As can be seen, if the window thickness and grid coverage were reduced to 0.05 μm and 5 percent, respectively, it would not be unreasonable to expect J_{sc} values exceeding 35 mA/cm^2.

Using 0.1 D/L for the AlGaAs-GaAs IRV and the values of the parameters in table II, we attempted to estimate the voltage and efficiency potential of this cell. The results are shown in table III. The low fill factor (FF) measured for this cell indicates a diode quality factor n greater than 1. The calculations, which assume a unity n value, indicate that the low FF has a depressing effect on

PRECEDING PAGE BLANK NOT FILMED

V_{oc}. If we give this cell a unity n value and a good fill factor, a V_{oc} of 1.040 V and an AMO efficiency of almost 21 percent result. Thus, merely by fabricating this cell with a decent fill factor, we could realize an efficiency two percentage points higher than has been achieved thus far. If we then reduce the AlGaAs window thickness to 0.05 μm and reduce the grid coverage to 5 percent, efficiency levels exceeding 23 percent should result.

We then performed essentially the same calculations for the P-base MIT cell number 8477 with its unpassivated emitter surface. As mentioned previously, this cell has an AlGaAs-GaAs interface at the "rear surface" that acts as a BSF layer. In the calculations, the same AlGaAs-GaAs IRV that we found for the Hughes cell (0.1 D/L) was used along with the values of the various parameters listed in table IV. As seen in table III, when the FF is raised to 0.86 the efficiency rises by about a point to 18.4 percent. If the emitter surface is then passivated (SRV = 0) and the anodic oxide AR coating is replaced by a dual layer coating, efficiencies comparable to those in the N-base cell are possible. It is evident that the critical need in this cell is the reduction of the emitter SRV.

To summarize, both the N-base and the P-base GaAs cells (in their planar configurations) have the potential to operate at AMO efficiencies between 23 and 24 percent. For the former the enabling technology is essentially in hand, while for the latter the problem of passivating the emitter surface remains to be solved.

THE GRATING CELL

A grating cell can be defined as a cell in which the junction (emitter) area has been reduced to a fraction of the total front (or rear) surface area. The purpose of going to a grating geometry is to secure an increase in voltage while maintaining (hopefully) a current level characteristic of a planar cell. The two simplest grating geometries are the stripe junction and the dot junction configurations. In the former the emitter is composed of an array of parallel stripes, and in the latter it is composed of an array of equally spaced dots.

Although previous theoretical analyses have indicated that the stripe grating geometry does not hold much promise for increased voltage (ref. 10), more recent calculations show that significant voltage gains are possible with the dot geometry (ref. 12). It has been shown that the effective base saturation current component of the dot grating cell decreases with the square root of the junction area. At the same time, because the emitter volume varies with the emitter area, the saturation current component from that region decreases linearly with junction area. A cell with a junction composed of an array of dots whose aggregate area is only 1 percent of the total cell area, for instance, would have its emitter component reduced by a factor of 100 and its base component reduced by a factor of 10 as compared to a planar cell with the same total area. The dot grating geometry thus has the potential for producing significant increases in cell voltage.

This concept is especially intriguing in the case of the P-base cell with its unpassivated emitter surface. In this case, the reduction of the N-type emitter surface area by several orders of magnitude would result in a cell almost completely bounded by passivatable P-type surfaces. The need to passivate the remaining N-type areas would be obviated by virtue of the relatively small contribution these areas would make to cell performance. Thus in the P-base cell the dot grating geometry is not only capable of producing a large decrease in J_0 but it also would eliminate essentially all of the hard-to-passivate N-type surfaces. The latter improvement

is a necessary, but, as we shall see, not a sufficient requirement for maintaining grating cell current levels comparable to those achieved in the planar cell.

We therefore calculated the efficiency of a 1 percent junction coverage, P-base dot grating cell using the MIT cell 8477 parameters (table IV) assuming planar cell current levels and a good FF. The results, according to table V, indicate that efficiencies in the 24.5 percent range are achievable.

Maintaining a high current level in a grating cell, however, requires more than just passivating the cell surfaces. It has been shown that to maintain full current capability in a grating cell, the base diffusion length must be much larger than the distance between junction areas in the grating structure[1] (ref. 10). If we assume that photolithographic limitations put a lower limit of 1 μm on the diameter of the emitter dots, then the smallest grating spacing possible for a cell with a 1 percent junction coverage would be 10 μm. This, unfortunately, is about the same magnitude as the diffusion lengths measured in most GaAs solar cells. In order to make use of the potential of the grating geometry a means would have to be found to raise L by at least an order of magnitude.

One way to obtain long diffusion lengths would be to go to a higher resistivity base material in which L values approaching 500 μm have been measured (refs. 13 to 15). Figure 2 summarizes measured hole and electron diffusion length data as a function of doping concentration. The problem with going to lower doping levels to achieve increased current is that one would expect (a priori) the base saturation current to rise precipitously, resulting in a serious decline in V_{oc}.

When one actually calculates the variation of efficiency with base doping level for the planar MIT cell 8477, however, it is found (fig. 3) that cell efficiency is surprisingly independent of base resistivity. In this plot J_{sc} and FF were assumed to be 29 mA/cm^2 and 0.86, respectively, while diffusion length data were taken from figure 2. Based on our previous analysis of the J_{sc} levels in the N-base cells, we have concluded that it is possible to reduce the AlGaAs-GaAs IRV to a level an order of magnitude below the diffusion velocity or lower. Measurements made by Nelson (ref. 16), although not made on solar cells, indicate that the IRV can in fact be two or three orders of magnitude less than D/L. We have therefore plotted the efficiency-doping relationship in figure 3 for several values of the IRV that bracket Nelson's measured 300 cm/sec (0.004 D/L) value (ref. 16).

The significance of figure 3 is that it shows that it should be possible to fabricate high efficiency GaAs solar cells with long (>200 μm) diffusion lengths. The fact that such a cell is possible indicates that we should be able to fabricate a high current, and thus a high efficiency, dot grating GaAs cell.

A few words should be said at this point concerning electrical contacts to the dot grating cell. Because of the large number of emitter dots that would be required, and because of the close spacing between them, the metallization making contact to the emitter areas on the front surface of the cell would probably shadow

---

[1]Unpublished data obtained from V.G. Weizer. An analysis of the dot-grating cell fabricated Swanson, et al. (ref. 11) indicates that this cell (with a diffusion length/grating-separation ratio of about 18) has an internal quantum efficiency close to 100 percent).

a significant portion of the cell front face. It thus appears that we would be forced to resort to an interdigitated back contact scheme such as that used by Swanson, et al. (ref. 11). This type of contacting, while being technically more difficult to achieve, does have the advantage of completely eliminating all shadowing effects. Thus, when we calculate the value of J_{sc} expected from a back contacted dot grating cell, we find that current levels over 36 mA/cm^2 are possible since the only losses are due to reflectivity and window absorption.

Figure 4 shows the calculated efficiency of a 1 percent junction coverage, back contacted dot grating cell as a function of base doping from $N = 1 \times 10^{15}$ cm^{-3} ($L = 200$ µm) to $N = 1 \times 10^{14}$ cm^{-3} ($L = 500$ µm). When the AlGaAs-GaAs IRV = 0, an efficiency of 25.3 percent is seen for a doping concentration of 1×10^{15} cm^{-3}. A penalty of about 1 percentage point is paid if the IRV is as high as 800 cm/sec (0.01 D/L).

The previous calculations were performed for a cell with a base width w of 2 µm. Since a change in w is expected to affect cell current and voltage in opposite directions, we should, by varying w, be able to observe an efficiency maximum at some optimum value of the base width. Figure 5 shows the variation of efficiency with w for the case where $N = 1 \times 10^{15}$ cm^{-3}. The efficiency is seen to be rather independent of base width for values above about 2 µm. When the IRV = 0, the efficiency peaks at about 25.7 percent at a base width of about 10 µm. For the higher value of the IRV a maximum of just over 25 percent occurs at a width of about 25 µm. Not only is the efficiency independent of the base width, it also becomes insensitive to the AlGaAs-GaAs IRV as the width is increased. As can be seen, high efficiency is maintained to thicknesses of 100 µm. This fact should facilitate the construction of this device since it would permit the use of thick cell fabrication techniques such as those employed by Swanson, et al. (ref. 11).

To summarize, both the N-base and the P-base GaAs cells in their planar configurations have the potential to operate at AMO efficiencies between 23 and 24 percent. For the former the enabling technology is essentially in hand, while for the latter the problem of passivating the emitter surface remains to be solved. In the dot grating configuration, P-base efficiencies approaching 26 percent are possible with minor improvements in existing technology. N-base grating cell efficiencies comparable to those predicted for the P-base cell are achievable if the N surface can be sufficiently passivated.

REFERENCES

1. Hovel, H.J.: Thickness. Semiconductors and Semimetals, Vol. 11, Solar Cells, Academic Press, 1975, Chapter 5, pp. 93-111.

2. Kamath, S.; Knechtli, R.C.; and Loo, R.: Fabrication of High Efficiency and Radiation Resistant GaAs Solar Cells. Solar Cell High Efficiency and Radiation Damage 1979, NASA CP-2097, 1979, pp. 209-216.

3. Knechtli, R.C.; Loo, R.Y.; and Kamath, G.S.: High-Efficiency GaAs Solar Cells. IEEE Trans. Electron Devices, vol. 31, no. 5, May 1984, pp. 577-588.

4. Werthen, J.G.: 18.7% Efficient (1-sun, AMO) Large-Area GaAs Solar Cells. Appl. Phys. Lett., vol. 46, no. 8, Apr. 15, 1985, pp. 776-778.

5. Sahai, R.: High Efficiency Thin Window $Ga_{1-x}Al_xAs$ - GaAs Solar Cells. 12th Photovoltaic Specialists Conference, IEEE, 1976, pp. 989-992.

6. Woodall, J.M.; and Hovel, H.J.: An Isothermal-Etchback Regrowth method for High Efficiency $Ga_{1-x}Al_xAs$ - GaAs Solar Cells. Appl. Phys. Lett., vol. 30, no. 9, May 1, 1977, pp. 492-493.

7. Yeh, Y.C.M.; Chang, K.I.; and Tandon, J.L.: Large Scale OM-CVD Growth of GaAs Solar Cells. 17th Photovoltaic Specialists Conference, IEEE, 1984, pp. 36-41.

8. Vernon, S.M.: Heteroepitaxial (Al)GaAs Structures on Ge and Si for Advanced High Efficiency Solar Cells. 17th Photovoltaic Specialists Conference, IEEE, 1984, pp. 434-439.

9. Yoshida, S.: Liquid Phase Epitaxy Technology of Large Area AlGaAs - GaAs Wafers of GaAs Solar Cells for Space Applications. 17th Photovoltaic Specialists Conference, IEEE, 1984, pp. 42-45.

10. Kong, Anthony K.; and Green, Martin A.: The Efficiency of Grating Solar Cells. J. Appl. Phys., vol. 49, no. 1, Jan. 1978, pp. 437-442.

11. Swanson, R.M.: Prime-Contact Silicon Solar Cells. IEEE Trans. Electron Devices, vol. 31, no. 5, May 1984, pp. 661-664.

12. Weizer, V.G.; and Godlewski, J.: Effect of Solar-Cell Junction Geometry on Open-Circuit Voltage, vol. 57, no. 6, Mar. 15, 1985, pp. 2292-2294.

13. Nelson, R.J.: Measurement of 100 μm Minority Carrier Diffusion Lengths in p-Gallium Arsenide by a New Photoluminescence Method. Gallium Arsenide and Related Compounds, C.M. Wolfe, ed., Inst. Physics Conf. Series No. 45, Bristol: Institute of Physics, 1979, pp. 256-262.

14. Ryan, R.D.; and Eberhardt, J.E.: Hole Diffusion Length in High Purity in n-GaAs. Solid State Electron., vol. 15, no. 8, Aug. 1972, pp. 865-868.

15. Sekela, A.M.; Feucht, D.L.; and Milnes, A.G.: Diffusion Length Studies in n-Gallium Arsenide. Gallium Arsenide and Related Compounds, C.M. Wolfe, ed., Inst. Physics Conf. Series No. 45, Bristol: Institute of Physics, 1979, pp. 245-253.

16. Nelson, R.J.: Interfacial Recombination in GaAlAs Heterostructures. J. Vac. Sci. Technol., vol. 15, no. 4, July/Aug. 1978, pp. 1475-1477.

TABLE I. - AM0 PERFORMANCE DATA

Cell	Reference	V_{oc}, V	J_{sc}, mA/cm^2	FF, percent	Efficiency, percent
N-base cells					
Hughes 2598	2	1.015	32.0	75.2	18.1
Hughes ED-31	3	1.024	30.0	84.0	19.0
Hughes 13610	(a)	1.031	28.4	78.2	16.7
Varian	4	1.012	30.5	81.8	18.7
Rockwell	5	.960	30.3	80.3	17.2
IBM	6	1.025	33.1	74.5	18.5
ASEC	7	1.004	28.0	80.0	16.6
Spire	8	[b]1.020	[b]28.3	85.3	[b]17.9
Mitsubishi	9	.990	31.4	80.1	18.4
P-base cells					
MIT 8477	(a)	1.036	28.7	79.0	17.3
Varian	4	.995	31.3	80.0	18.4

[a]Unpublished data obtained at NASA Lewis Research Center.
[b]Estimated AM0 values.

TABLE II. - N-BASE CELL PARAMETERS: HUGHES CELL 2598

Parameter	Base	Emitter
L, μm	5	10
D, cm^2/sec	6	77
d, μm	10	0.5
N, cm^{-3}	10^{17}	10^{18}
S, cm/sec	10^4	8×10^3
n_i, cm^{-3}	2×10^6	2×10^6

TABLE III. - CALCULATED AMO PERFORMANCE PARAMETERS

	J_{sc}, mA/cm^2	V_{oc}, V	FF, percent	Efficiency, percent
Hughes cell 2958				
Experimental data	32.0	1.015	75.2	18.1
Optimized fill factor	31.96	1.040	86.0	20.9
Window, grid optimized	35.77	1.043	86.0	23.4
MIT cell 8477				
Experimental data	28.7	1.036	79.0	17.3
Optimized fill factor	28.30	1.034	86.0	18.4
SRV optimized, DLAR	34.94	1.061	86.0	23.3

TABLE IV. - P-BASE CELL PARAMETERS: MIT CELL 8477

Parameter	Base	Emitter
L, μm	20	0.5
D, cm^2/sec	121	3
d, μm	2	0.07
N, cm^{-3}	10^{17}	$5x10^{18}$
S, cm/sec	0	10^7
n_i, cm^{-3}	$2x10^6$	$2x10^6$

TABLE V. - P-BASE CELL PERFORMANCE: MIT CELL 8477

	J_{sc}, mA/cm^2	V_{oc}, V	FF, percent	Efficiency, percent
Optimized fill factor	28.30	1.034	86	18.4
1-Percent dot grating	(35.00)	1.118	86	24.5

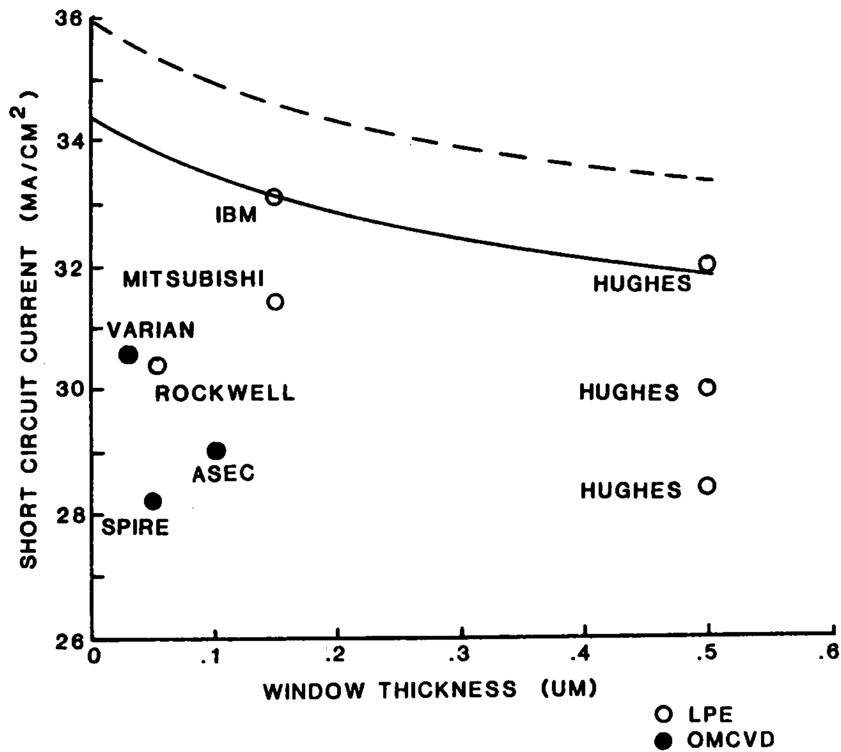

Figure 1. - A Plot of measured AMO short circuit current density vs AlGaAs window thickness.

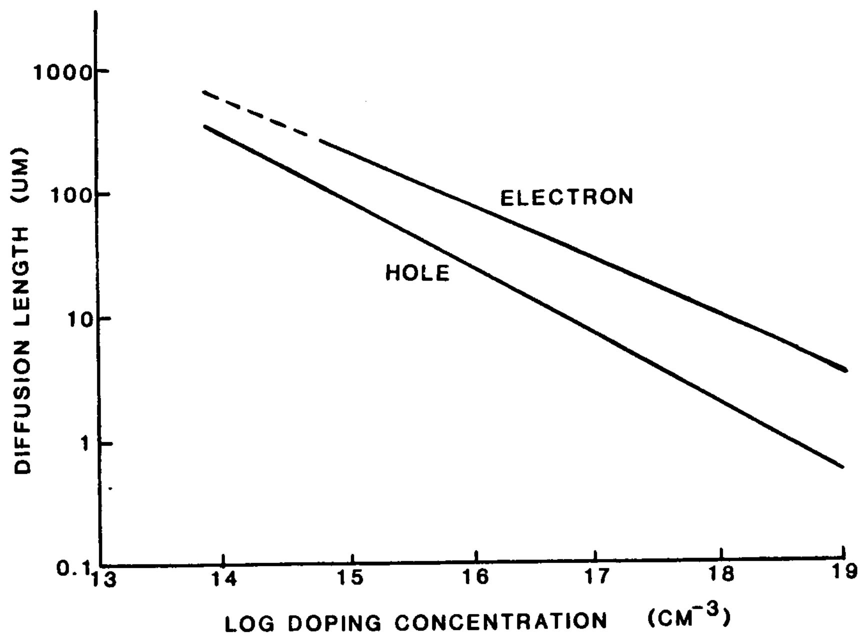

Figure 2. - Electron and hole diffusion lengths as function of doping concentration.

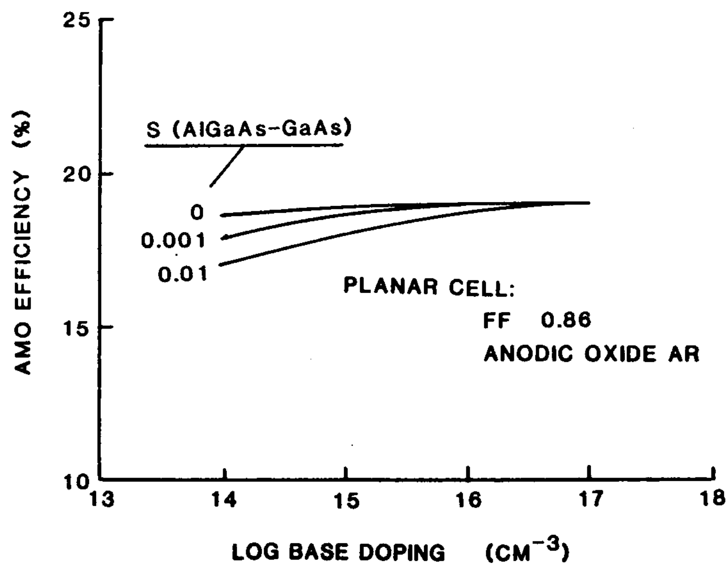

Figure 3. - Variation of P-base GaAs cell AMO efficiency with base doping level.

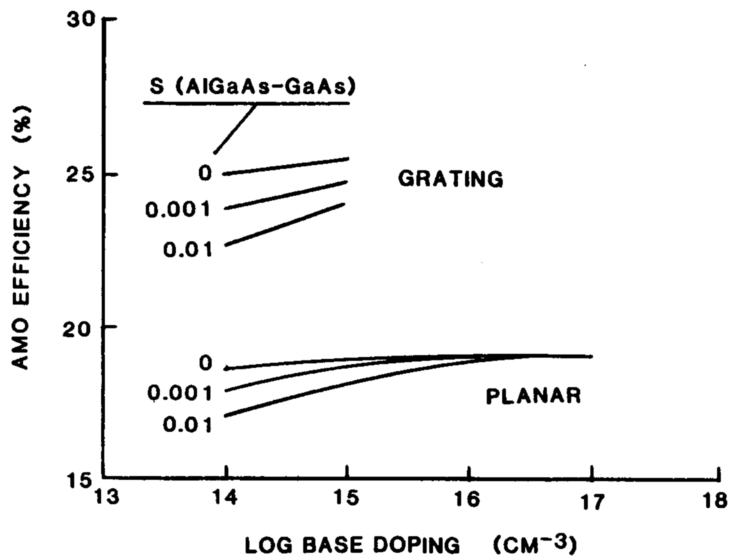

Figure 4. - Variation of P-base GaAs cell AMO efficiency with base doping level, planar vs 1 percent dot geometry.

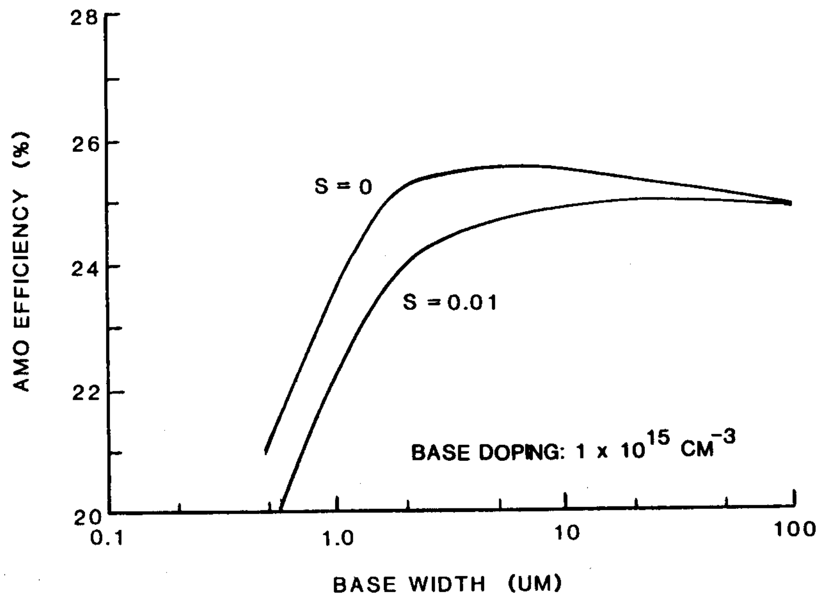

Figure 5. - Variation of P-base GaAs cell AMO efficiency with base width.